





Topological invariants of Floquet topological phases under periodical drivingKai-Ye Shi ¹, Rui-Qi Chen ¹, Shuaining Zhang ^{1,2,*} and Wei Zhang ^{1,2,3,†}¹*Department of Physics, Renmin University of China, Beijing 100872, China*²*Beijing Academy of Quantum Information Sciences, Beijing 100193, China*³*Beijing Key Laboratory of Opto-electronic Functional Materials and Micro-nano Devices, Renmin University of China, Beijing 100872, China*

(Received 15 February 2022; accepted 19 October 2022; published 1 November 2022)

Owing to the replication of Floquet bands and the presence of additional gaps in the quasienergy dimension, the topological phases in a periodically driven system cannot be fully characterized by the conventional topological invariants used in static systems. In particular, an anomalous strong topological phase can be a host in driven systems, featured by nontrivial counterpropagating edge modes which cannot be characterized by the bulk band structure. In this paper, we propose a scheme to obtain a complete characterization of Floquet topological phases using only information about bulk dispersions under the condition that both the location and chirality of Floquet band-touching points are not changed by the periodical driving. A set of topological invariants associated with the band-touching points are formulated to establish a one-to-one correspondence to the number of edge modes. Finally, we discuss the experimental realization and detection scheme using cold atomic gases.

DOI: [10.1103/PhysRevA.106.053301](https://doi.org/10.1103/PhysRevA.106.053301)**I. INTRODUCTION**

The study of topological phases [1,2] has been one of the most important frontiers of physics over the past several decades since they not only surpass the conventional quantum phase-transition paradigm of spontaneous symmetry breaking but also have potential applications in quantum transport [3–5] and quantum computation [6,7]. Of particular interest are symmetry-protected topological (SPT) phases, which are gapped quantum phases protected by the symmetries of the system [8–11]. As a well-known example of SPT phases, topological insulators feature short-range quantum entanglement and a pair of counterpropagating helical boundary modes which can flow without backscattering as long as the time-reversal symmetry is preserved [12–14]. For general cases, much effort has been devoted to the search for topological invariants which can distinguish various topological phases under different symmetries [15,16] and to establish a direct relation between topological invariants of the bulk spectrum and gapless edge modes known as the bulk-boundary correspondence (BBC) [17,18].

Recently, topological phases and their characterization in periodically driven systems have attracted a great deal of attention both theoretically [19–25] and experimentally [26–29]. One of the most intriguing motivations is to search for novel topological states beyond the scope of static systems. Owing to the periodicity in the temporal dimension, one can define a Floquet Brillouin zone (FBZ) in the frequency domain, and the dispersion of the system is duplicated to form quasienergy bands. When the quasienergy spectra with

different band indices cross, a gap can be opened, and the system may enter a new phase.

There are, in general, two types of driving schemes to realize a Floquet system: (1) the driving sequence is composed of various topologically trivial Hamiltonians, and the effective Floquet Hamiltonian does not acquire any additional symmetry other than spatial translation [19,26–29]; (2) the periodic driving is realized by varying some parameters of a specific static Hamiltonian with all symmetries preserved [20,23,25,30,31]. For the first type of driving, previous studies suggest the emergence of a new type of topological phase, referred to as anomalous Floquet topological phases [19,24], which cannot be described by topological invariants defined for static systems. For example, robust edge modes can exist in two-dimensional (2D) Floquet systems while the Chern number of all bands are zero, clearly violating the conventional BBC. In order to solve this issue, some proposals have been made to describe the Floquet topological phases with winding numbers [19], topological singularities of phase bands [32] defined in the momentum-time space, or $(d - 1)$ -dimensional band inversion surfaces [30]. The second type of driving protocol is more exotic as it can host nontrivial counterpropagating edge states, which can originate from either strong topology [25] or weak topology [20,31]. Notably, the aforementioned frameworks of topological characterization cannot fully identify the emergence and number of such edge modes. Although a certain form of scattering matrix invariant has been defined to meet this goal [31], a topological invariant determined solely by the band structure in spatial dimensions is still lacking.

Here, we propose a systematic protocol to construct topological invariants for Floquet systems under the condition that the band-touching points of the Floquet bands have the same position and chirality as in the static model at topolog-

*zhangshuaining@ruc.edu.cn

†wzhangl@ruc.edu.cn

ical phase transitions. Such requirements are often naturally satisfied [23,25,30] for the second type of driving with all symmetries preserved and thus can work for exotic topological phases presenting counterpropagating edge modes. This method is based on the classification and characterization of topological phases in a static system. By turning on periodic driving and increasing the driving period, quasienergy bands with different indices will cross to open new gaps. Since the position and chirality of these band-touching points remain the same, topological invariants can be defined by generalizing the corresponding definition in static models for these quasienergy gaps, and the Floquet topological phase is completely characterized by the topological invariants of all gaps. As an example, we study a Floquet system by driving the quantum anomalous Hall effect (QAHE) model in a 2D square lattice [33–35], where robust counterpropagating edge modes can exist even when the Chern number and winding numbers are all zero. This phase, referred to as the type-II anomalous Floquet topological (AFT-II) phase in the following discussion, is a strong topological phase and beyond the characterization of the winding number [19] or topological singularities of phase bands [32]. However, we show that such an exotic phase can be characterized by the topological invariants proposed here. Finally, we discuss possible detection methods in the context of cold atomic gases. We stress that our scheme requires only information about the bulk Floquet bands and not the time evolution in the temporal domain or the scattering matrix invariants.

The remainder of this paper is organized as follows. In Sec. II, we present the definition of topological invariants for a general Floquet system satisfying the two requirements of band-touching points. To demonstrate the validity of the characterization scheme, we discuss in Sec. III its implementation in a driving QAHE model, where an AFT-II phase is identified and fully characterized. An exact bulk-boundary correspondence can be obtained between these edge modes and the newly defined topological invariants, such that the BBC is reestablished. In Sec. IV, we introduce a realization of such a 2D QAHE model in cold atomic gases and propose a feasible detection scheme based on existing techniques. Finally, we summarize in Sec. V.

II. GENERALIZATION OF TOPOLOGICAL INVARIANTS TO FLOQUET BANDS

For a time-periodic system $\hat{H}(t) = \hat{H}(t + T)$ with period T , the energy is no longer conserved, and its symmetry group is the time-shifted group \mathcal{T} [36]. The irreducible representation of \mathcal{T} defines a quasienergy ε which plays the same role as energy in static systems. Similar to the quasimomentum in spatial dimensions, the quasienergy is also regarded as a periodic variable defined in the first FBZ $(-\pi/T, \pi/T]$ and has an infinite number of copies; that is, ε is equivalent to $\varepsilon + 2n\pi/T$ for an arbitrary band index n . The Floquet quasienergy spectra are characterized by the effective Hamiltonian $\hat{H}_F = i \ln \hat{U}_T / T$, where $\hat{U}_T = \hat{\mathbb{T}} e^{-i \int_0^T \hat{H}(t) dt}$ is the evolution operator, with $\hat{\mathbb{T}}$ being the time-ordering operator. Floquet topological phases can consequently be defined based on the quasienergy spectra and will acquire characteristics without a static counterpart because of the discrete translational symmetry in the

temporal domain. Specifically, an alternative type of gap referred to as the π -gap will emerge at the boundary of the first FBZ at $\varepsilon = \pm\pi/T$. Band crossing at the π -gap can lead to the anomalous Floquet topological phase, which hosts robust edge modes with the Chern numbers of all bands being zero [19]. Thus, the Chern number can no longer describe the number of edge states and has to be replaced or supplemented by other topological invariants.

For the first type of driving, since there are no additional symmetries, the Floquet topological phases spawned therein can be fully described by the winding number $w_{m=0,\pi}$ of the m -gap, which corresponds to the net number of edge modes [19]. A detection method for these winding numbers has been proposed [37] and successfully implemented in cold atomic systems [29]. For the second type of driving, however, the instantaneous Hamiltonian $\hat{H}(t)$ preserves the same symmetry as the original static model, which makes the Floquet system also inherit the full symmetries. In this case, counterpropagating edge modes can be realized and protected by topology [25], and the winding numbers can no longer identify the emergence and number of edge modes. In this case, the BBC needs to be further modified.

To fulfill this goal, we recall that a topological phase transition is related to the closing and reopening of energy bands. A richer topological phase diagram can be expected in Floquet systems since the periodicity of Floquet bands will lead to additional band-touching points. In the limit of $T \rightarrow 0$, the periodicity of quasienergy bands tends to infinity, and the Floquet band structure is equivalent to the static counterpart. The topological properties of such a case can be characterized by conventional topological invariants $\{v^s\}$ defined for static models. By increasing T , the quasienergy bands with higher band indices will extend into the first FBZ to induce new band crossings. Since the Floquet Hamiltonian preserves all symmetries of the static model, the two following conditions are often satisfied, e.g., in a driven system with particle-hole symmetry [23,25,30]:

- (1) The momentum k^c of band-touching points at topological phase transitions is the same as those in the static system.
- (2) Floquet engineering does not alter the chirality of these band-touching points.

Under these conditions, new topological phases will emerge, and the corresponding topology should be captured by some new topological invariants $\{v^d\}$. The complete topological characterization of the Floquet bands is jointly determined by $\{v^s, v^d\}$. Since the driving-induced topological invariants $\{v^d\}$ are directly caused by the replication and translation of quasienergy bands over different FBZs, one would naturally expect that $\{v^d\}$ satisfy the same law as $\{v^s\}$ for the static band structure. In other words, $\{v^d\}$ are just the replication of $\{v^s\}$, but for the crossing of bands of different FBZs.

III. IMPLEMENTATION IN A DRIVING QAHE MODEL

In this section, we implement the general protocol outlined in the previous section for a periodically driven QAHE model in a 2D square lattice. To give a complete picture, we first briefly review the topological invariants of a static model and present the generalization to a driving system. Finally,

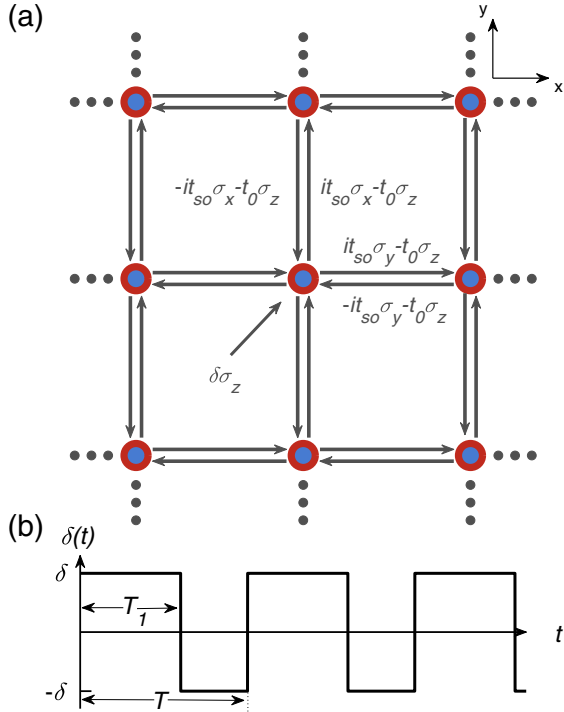


FIG. 1. (a) Illustration of the QAHE model in a 2D square lattice. The corresponding Bloch Hamiltonian is given in Eq. (2). (b) A two-stage driving scheme in the form of a step function is considered to give the analytic results of topological phase transitions.

we consider as an example a two-stage driving sequence and discuss the resulting Floquet topological phases.

A. Topological invariants in a static QAHE model

The static 2D QAHE model, as illustrated in Fig. 1(a), has been experimentally realized and thoroughly investigated in cold atomic gases [33–35]. The Hamiltonian can be expressed in Bloch form as

$$\mathcal{H}(\mathbf{k}) = \mathbf{h}(\mathbf{k}) \cdot \boldsymbol{\sigma}, \quad (1)$$

where $\mathbf{h}(\mathbf{k}) = (2t_{so} \sin k_y, 2t_{so} \sin k_x, \delta - 2t_0(\cos k_x + \cos k_y))$. The Hamiltonian has particle-hole symmetry $\mathcal{C}\mathcal{H}(\mathbf{k})\mathcal{C}^{-1} = -\mathcal{H}(-\mathbf{k})$, with $\mathcal{C} = \sigma_x K$ and $\mathcal{C}^2 = +1$, where σ_x is the x Pauli matrix and K is the complex-conjugation operator. This model belongs to the D class in the Altland-Zirnbauer (AZ) classification [15], and the topological characterization is described by a \mathbb{Z} invariant (first Chern number) [16,38,39],

$$C_{l=\pm} = \frac{i}{2\pi} \int_{1\text{BZ}} \text{Tr}[P_l dP_l \wedge dP_l]. \quad (2)$$

Here, $P_l(\mathbf{k}) = |\psi_l(\mathbf{k})\rangle \langle \psi_l(\mathbf{k})|$, $|\psi_l(\mathbf{k})\rangle$ is the eigenstate of the l th band, and the summation runs over the first Brillouin zone (1BZ) in quasimomentum space. A direct calculation gives the Chern number of the lower band as $C_- = \text{sgn}(\delta)$ when $|\delta| < 4t_0$ (assuming $t_0 > 0$ without loss of generality) and $C_- = 0$ otherwise.

The QAHE model is invariant under inversion symmetry defined by $\mathcal{P} = \hat{P} \otimes \hat{R}$, where $\hat{P} = \sigma_z$ and \hat{R} is the spa-

tial reflection operator which transforms the Bravais lattice vector $R \rightarrow -R$. By establishing a natural correspondence between the time-reversal-invariant topological insulator and the QAHE model, the topological phases of the QAHE model can be revealed by a \mathbb{Z}_2 invariant ν defined as [40]

$$(-1)^\nu = \prod_i \xi_-(\Lambda_i), \quad (3)$$

where $\xi_-(\Lambda_i) = \langle u_-(\Lambda_i) | \hat{P} | u_-(\Lambda_i) \rangle$ represents the equilibrium spin polarization of the lower-band Bloch states at the four high-symmetry points $\Lambda_i = \{\Gamma, M, X_{1,2}\}$ in the 1BZ and $|u_-(\Lambda_i)\rangle$ are the Bloch states of the lower band. The phase with $\nu = 0$ corresponds to a trivial topology, and the phase with $\nu = 1$ corresponds to a nontrivial topology. The Chern number of the lower band can be further expressed as [34,35,40]

$$C_- = -\frac{\nu}{2} \sum_i \xi_-(\Lambda_i). \quad (4)$$

Since $\mathcal{H}(X_1) = \mathcal{H}(X_2)$, Eq. (3) has an equivalent form:

$$(-1)^\nu = \text{sgn}[E_d(\Gamma)E_d(M)], \quad (5)$$

where E_d represents the energy of the spin-down band and takes values of $E_d(M) = -\delta - 4t_0$ and $E_d(\Gamma) = -\delta + 4t_0$ at the M and Γ points, respectively. From this expression, one can easily observe that the nontrivial topology is induced by the inversion of spin bands, which is just the physical mechanism of the quantum anomalous Hall effect. The inversion of spin bands leads to a ring structure in Brillouin zones referred to as a band inversion surface (BIS) [41], which is composed of points satisfying $\xi_-(\mathbf{k}) = 0$ and reflects the topological properties of the system [35]. Within the topologically nontrivial region with $\nu = 1$, one can still distinguish two phases with different Chern numbers ($C_- = +1$ and $C_- = -1$) based on the position of the BIS in momentum space. In fact, according to Eq. (4), we can equivalently express the Chern number as the difference between two \mathbb{Z}_2 invariants as

$$C_- = \nu^\Gamma - \nu^M,$$

$$(-1)^{\nu^\Gamma} = \text{sgn}[E_d(\Gamma)E_d(X)], \quad (6)$$

$$(-1)^{\nu^M} = \text{sgn}[E_d(M)E_d(X)],$$

where $E_d(X) \equiv E_d(X_1) = E_d(X_2) = -\delta$. The phase with $C_- = +1$ corresponds to the choice of ($\nu^\Gamma = 1, \nu^M = 0$), which indicates that the band crossing takes place between the X and Γ points and a BIS exists around Γ . On the other hand, the phase with $C_- = -1$ corresponds to ($\nu^\Gamma = 0, \nu^M = 1$), and the spin bands overlap between the X and M points with a BIS surrounding M .

For the static QAHE model, the bands contact at energy $E = 0$, i.e., $|\mathbf{h}(\mathbf{k})| = 0$. Thus, a topological phase transition will occur when

$$E_d(\Lambda_i) = 0. \quad (7)$$

The chirality of the band-touching points can be calculated as [23]

$$\text{Ch}(\mathbf{k}) = \text{sgn}[\partial_{k_x} \mathbf{h}(\mathbf{k}) \times \partial_{k_y} \mathbf{h}(\mathbf{k})]_z. \quad (8)$$

It is not difficult to obtain $\text{Ch}(\Gamma) = \text{Ch}(M) = -1$ and $\text{Ch}(X_1) = \text{Ch}(X_2) = +1$. Thus, when the band gap closes and reopens at the Γ (or M) point, the Chern number would change by $\Delta C_-(\Gamma) = \text{Ch}(\Gamma)\delta h_z(\delta_c + d\delta \rightarrow \delta_c - d\delta) = +1$ [or $\Delta C_-(M) = \text{Ch}(M)\delta h_z(-\delta_c - d\delta \rightarrow -\delta_c + d\delta) = -1$], with $\delta_c = 4t_0$, and a pair of edge modes with positive (negative) chirality will appear at $k = 0$ ($k = \pi$).

B. Topological invariants in a periodically driven QAHE model

With the analysis of static systems, next, we impose periodic driving by varying the parameters of the 2D QAHE model. For the convenience of experimental realization, we consider a time-dependent Zeeman shift $\delta(t) = \delta(t + T)$, which can be implemented by varying the detuning of the Raman process between the two pseudospin states in cold atomic gases [33–35]. Since $\delta(t)$ is a periodic function of T , it can always be expanded into a superposition of trigonometric functions, i.e., $\delta(t) = \delta_0 + V(t)$, where $\delta_0 = \int_0^T \delta(t)dt/T$ and $V(t) = \sum_\ell [a_\ell \sin(\ell\omega t) + b_\ell \cos(\ell\omega t)]$, with $a_\ell = (2/T) \int_0^T \delta(t) \sin(\ell\omega t)dt$ and $b_\ell = (2/T) \int_0^T \delta(t) \cos(\ell\omega t)dt$. Here, we define $\omega = 2\pi/T$. The time-dependent Hamiltonian can then be written as

$$\mathcal{H}(\mathbf{k}, t) = \mathcal{H}_s(\mathbf{k}) + \hat{V}(t), \quad (9)$$

where the static component $\mathcal{H}_s(\mathbf{k}) = \mathbf{h}_s(\mathbf{k}) \cdot \boldsymbol{\sigma}$, with $\mathbf{h}_s(\mathbf{k}) = (2t_{s0} \sin k_y, 2t_{s0} \sin k_x, \delta_0 - 2t_0(\cos k_x + \cos k_y))$, and $\hat{V}(t) = V(t)\sigma_z$ is the driving term which changes periodically over time.

First, we show this periodically driven system satisfies the two conditions of band-touching points. For an arbitrary form of periodic driving, we can choose a certain time $t' \in (0, T)$ to divide a full period into two parts labeled $\mathcal{H}_1(\mathbf{k}, t)$ for $t \in [0, t')$ and $\mathcal{H}_2(\mathbf{k}, t)$ for $t \in [t', T)$. According to Ref. [23], if $\mathcal{H}_1(\mathbf{k}, t) = \mathcal{H}_1(\mathbf{k})$ and $\mathcal{H}_2(\mathbf{k}, t) = \mathcal{H}_2(\mathbf{k})$ are both time-independent, one can prove that the Zeeman fields in \mathcal{H}_1 and \mathcal{H}_2 are parallel at the momenta \mathbf{k}^c where two bands touch at a topological phase-transition point, i.e., $\mathbf{h}_1(\mathbf{k}^c) \parallel \mathbf{h}_2(\mathbf{k}^c)$. Considering the identity

$$(\mathbf{h}_1 \cdot \boldsymbol{\sigma})(\mathbf{h}_2 \cdot \boldsymbol{\sigma}) = \mathbf{h}_1 \cdot \mathbf{h}_2 + i\boldsymbol{\sigma} \cdot (\mathbf{h}_1 \times \mathbf{h}_2), \quad (10)$$

one can easily find that $[\mathcal{H}_1(\mathbf{k}^c), \mathcal{H}_2(\mathbf{k}^c)] = 0$. In addition, since the effective Floquet Hamiltonian reads $\mathcal{H}_F(\mathbf{k}) = (i/T) \ln \hat{\mathbb{T}} e^{-i \int_0^T \mathcal{H}(\mathbf{k}, t) dt}$, we get

$$\begin{aligned} \mathcal{H}_F(\mathbf{k}^c) &= \frac{\mathcal{H}_1(\mathbf{k}^c)t' + \mathcal{H}_2(\mathbf{k}^c)(T - t')}{T} \\ &\equiv \mathbf{h}_F(\mathbf{k}^c) \cdot \boldsymbol{\sigma}; \end{aligned} \quad (11)$$

hence, $\mathbf{h}_1(\mathbf{k}^c) \parallel \mathbf{h}_2(\mathbf{k}^c) \parallel \mathbf{h}_F(\mathbf{k}^c)$ are all parallel, giving $[\mathcal{H}_F(\mathbf{k}^c), \mathcal{H}_{j=1,2}(\mathbf{k}^c)] = 0$.

In general cases where $\mathcal{H}_1(\mathbf{k}, t)$ and $\mathcal{H}_2(\mathbf{k}, t)$ vary over time, we can define their corresponding effective Floquet Hamiltonians

$$\begin{aligned} \mathcal{H}'_{1,F}(\mathbf{k}) &= \frac{i}{t'} \ln \hat{\mathbb{T}} e^{-i \int_0^{t'} \mathcal{H}_1(\mathbf{k}, t) dt}, \\ \mathcal{H}'_{2,F}(\mathbf{k}) &= \frac{i}{T - t'} \ln \hat{\mathbb{T}} e^{-i \int_{t'}^T \mathcal{H}_2(\mathbf{k}, t) dt}, \end{aligned} \quad (12)$$

which by definition are time independent and can give the same stroboscopic time evolution as $\mathcal{H}_1(\mathbf{k}, t)$ and $\mathcal{H}_2(\mathbf{k}, t)$. Thus, the effective Zeeman fields $\mathbf{h}'_{1,F}(\mathbf{k}^c)$ and $\mathbf{h}'_{2,F}(\mathbf{k}^c)$ associated with $\mathcal{H}'_{1,F}$ and $\mathcal{H}'_{2,F}$ also satisfy the relation $\mathbf{h}'_{1,F}(\mathbf{k}^c) \parallel \mathbf{h}'_{2,F}(\mathbf{k}^c) \parallel \mathbf{h}_F(\mathbf{k}^c)$. Since the division is arbitrarily made, for another time $t'' > t'$, we can also get $\mathbf{h}'_{1,F}(\mathbf{k}^c) \parallel \mathbf{h}'_{2,F}(\mathbf{k}^c) \parallel \mathbf{h}_F(\mathbf{k}^c)$. Thus, we can conclude that $\mathbf{h}'_{1,F}(\mathbf{k}^c) \parallel \mathbf{h}''_{1,F}(\mathbf{k}^c)$ and $[\mathcal{H}'_{1,F}(\mathbf{k}^c), \mathcal{H}''_{1,F}(\mathbf{k}^c)] = 0$. Recalling the definition of $\mathcal{H}'_{1,F}$,

$$e^{-i\mathcal{H}'_{1,F}(\mathbf{k}^c)t''} = e^{-i \int_{t'}^{t''} \mathcal{H}(\mathbf{k}, t) dt} e^{-i\mathcal{H}'_{1,F}(\mathbf{k}^c)t'}, \quad (13)$$

and taking the limit $t'' \rightarrow t'$, we obtain the relation $[\mathcal{H}(\mathbf{k}^c, t'), \mathcal{H}'_{1,F}(\mathbf{k}^c)] = 0$ and, consequently, $\mathbf{h}(\mathbf{k}^c, t') \parallel \mathbf{h}_F(\mathbf{k}^c)$ for arbitrary time t' . This leads to the conclusion that $[\mathcal{H}(\mathbf{k}^c, t_1), \mathcal{H}(\mathbf{k}^c, t_2)] = 0$ for all $t_1 \neq t_2$, which gives $[\mathcal{H}_s(\mathbf{k}^c), \hat{V}(t)] = 0$. Thus, the band-touching point $\mathbf{k}^c \in \{\Lambda_i\}$ at the topological phase transition is also a high-symmetry point regardless of the specific form of $V(t)$, and condition 1 introduced in Sec. II is satisfied.

In addition, since $\int_0^T V(t)dt = 0$, an analysis similar to that in Ref. [23] shows that a topological phase transition would occur when the following condition is satisfied:

$$E_d^s(\Lambda_i) = n\pi/T. \quad (14)$$

Here, E_d^s is the eigenvalue of the spin-down band of the steady-state Hamiltonian \mathcal{H}_s . We can see that when $T \rightarrow 0$, Eq. (14) reduces to its static counterpart, Eq. (7). This means that in the high-frequency limit, the Floquet system behaves as a static model. With increasing T , more Floquet bands with different n 's can fulfill the condition of Eq. (14), and multiple topological phase transitions will take place. We then notice that the time-dependent Hamiltonian $\mathcal{H}(t)$ also preserves the C_4 symmetry $(k_x, k_y; \sigma_x, \sigma_y) \rightarrow (k_y, -k_x; -\sigma_y, \sigma_x)$. Thus, the Floquet bands also have C_4 symmetry, which protects the chirality of the band-touching points and condition 2 in Sec. II is satisfied. As a result, the chirality of the band-touching points is related to only the high-symmetry points and is independent of the value of n . Since both conditions 1 and 2 introduced in Sec. II are satisfied, these emerging Floquet topological phases can be characterized by generalizing the discussion of static systems. We emphasize that the existence of C_4 symmetry is sufficient, but not necessary, to validate condition 2. In fact, by selecting an appropriate driving sequence, condition 2 can be satisfied even if $\hat{H}(t)$ has no C_4 symmetry [25].

For illustration purposes, we consider as an example a two-stage driving scheme in the form of a step function:

$$\delta(t) = \begin{cases} \delta, & t \in [\ell T, \ell T + T_1), \\ -\delta, & t \in [\ell T + T_1, (\ell + 1)T), \end{cases} \quad \ell \in \mathbb{N}, \quad (15)$$

with $T_1 \in (0, T)$, as illustrated in Fig. 1(b). We stress that this specific choice is made to simplify the derivation such that an analytic solution can be obtained. The qualitative conclusions, including the emergence and characterization of novel topological phases, will not be changed if a more general driving protocol is employed. This driving method will not destroy the particle-hole symmetry of the static system, and Floquet bands will inherit the symmetry. As pointed in Ref. [25], a periodically driven system with particle-hole symmetry would host counterpropagating edge modes with positive and negative chiralities fixed, respectively, at $k = 0$

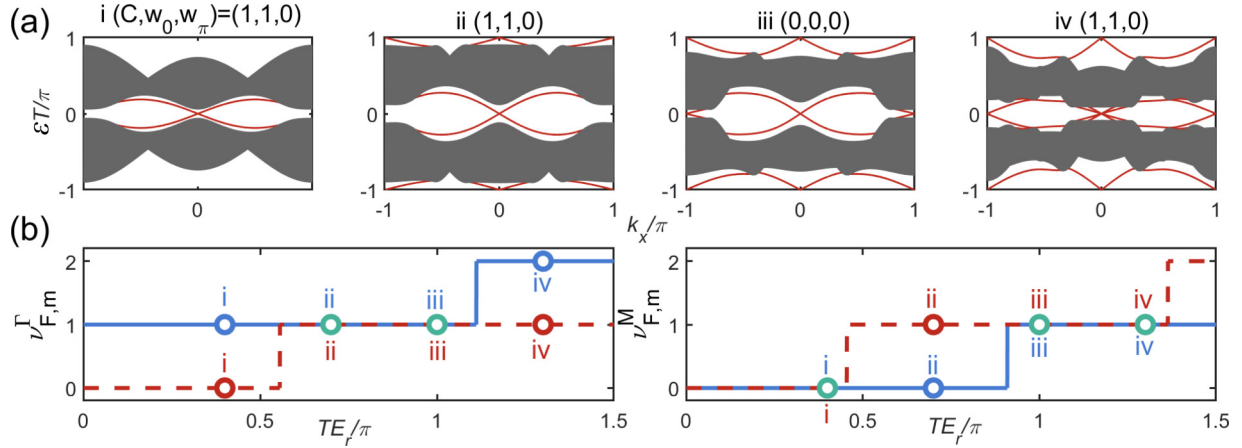


FIG. 2. Quasienergy spectra and topological invariants. (a) Quasienergy spectra in the first FBZ. The driving period T is $0.4\pi/E_r$ in panel (i), $0.7\pi/E_r$ in panel (ii), $1.0\pi/E_r$ in panel (iii), and $1.3\pi/E_r$ in panel (iv), where E_r is the recoil energy associated with the lattice. Notice that in the phase shown in panel (iii), robust edge modes (red solid curves) are present when both the Chern number C_- and winding numbers $w_{0,\pi}$ are zero. (b) The topological invariants $v_{F,m}^\Gamma$ (left panel) and $v_{F,m}^M$ (right panel) for the four phases depicted in (a). The blue solid and red dashed lines represent the cases of $m = 0$ and $m = \pi$, respectively. Other parameters used are $t_0/E_r = 0.5$, $t_{s0}/E_r = 0.25$, $T_1/T_2 = 3/2$, and $\delta/E_r = 1$

and $k = \pi$; hence, they are prevented from backscattering. The emergence of such chiral edge modes makes the winding number insufficient to fully characterize the topology of the underlying system. As shown in Fig. 2(a), phases i, ii, and iv have exactly the same Chern number and winding number, but their associated edge state spectra are different. Of particular interest is phase iii, which has both the Chern number of lower band and winding numbers equal to zero but presents robust edge states. To distinguish it from the anomalous Floquet topological phase discussed in Refs. [19,24], we denote phase iii as an AFT-II to emphasize that the edge states cannot be described by winding numbers. It is worth noting that the AFT-II phase discussed here is a strong topological phase owing to the particle-hole symmetry [25].

Next, we show that the AFT-II phase can be characterized by constructing new topological invariants via the method introduced in Sec. II. We first need to find the contact conditions of the Floquet bands. Thanks to the simplicity of the two-stage driving scheme (15), an analytic expression for the topological phase-transition point can be obtained [23]:

$$\frac{T_1\delta - T_2\delta}{T} - 2t_0(e^{i\alpha} + e^{i\beta}) = \frac{n\pi}{T}, \quad (16)$$

where $T_2 = T - T_1$ and $\alpha, \beta = \{0, \pi\}$. The contact points of Floquet bands also locate at the high-symmetry points. The chirality of the band-touching points can also be calculated analytically, leading to $\text{Ch}(\Gamma) = \text{Ch}(M) = -1$ and $\text{Ch}(X_1) = \text{Ch}(X_2) = +1$, which are identical to the static model. This allows us to extend Eq. (6) to the n th Floquet band,

$$\begin{aligned} v_n &= v_n^\Gamma - v_n^M, \\ (-1)^{v_n^\Gamma} &= \text{sgn}[E_{nd}^s(\Gamma)E_{nd}^s(X)], \\ (-1)^{v_n^M} &= \text{sgn}[E_{nd}^s(M)E_{nd}^s(X)], \end{aligned} \quad (17)$$

where $E_{nd}^s = E_d^s - n\pi/T$. By comparing (17) with Eq. (6) of the static system, we can see that the influence of Floquet engineering on the QAHE model is only to expand the energy

of band-touching points from the 0-gap to quasienergies of $n\pi/T$.

To see this more clearly, we choose the parameters of phase iii in Fig. 2(a) and show in Fig. 3(a) the Floquet band spectra along the M - Γ - M line of the 2D Brillouin zone, where the n th spin-up (red) and spin-down (blue) bands are obtained by copying and translating by $n\pi/T$ from their corresponding static bands (solid lines). Within the first FBZ ($-\pi/T, \pi/T$] (shaded area), four band inversion points can be identified and are labeled by circles. At point c, the band inversion occurs at the 0-gap between the zeroth spin-down band (blue 0) and the zeroth spin-up band (red 0), which is also present in static systems. Point b (point d) represents a band crossing between the blue 0 and red 1 (red -1) occurring at the π -gap. The inversion of bands at point e labels the crossing of the blue 1 and red -1 bands, which can also be obtained by the crossing of blue 0 and red -2 at point \tilde{e} , owing to the periodicity of the Floquet bands.

With a finite t_{s0} , the band inversion points b, c, d, and e will open topological gaps as depicted respectively in Figs. 3(b)–3(e). According to Eq. (17), we can get $v_1^\Gamma = v_0^\Gamma = v_{-1}^M = v_{-2}^M = 1$, while the other $v_n^{\Gamma,M}$ are zero. By counting all gaps within the first FBZ, we can reach a set of new topological invariants for Floquet topological phases,

$$\begin{aligned} v_{F,m} &= v_{F,m}^\Gamma - v_{F,m}^M, \\ v_{F,m}^\Lambda &= \sum_k v_{2k+\delta_{m,\pi}}^\Lambda, \end{aligned} \quad (18)$$

where $m = \{0, \pi\}$ and $\Lambda = \{\Gamma, M\}$. The topological invariant $v_{F,m}^\Gamma$ ($v_{F,m}^M$) represents the number of edge modes with positive (negative) chirality in the m -gap, while $v_{F,m}$ gives the net number of edge modes therein and is equivalent to the winding number w_m . To this end, the chirality and number of edge states of the Floquet system can be well captured by using the topological invariants $v_{F,m}^\Lambda$, as illustrated in Figs. 2(b), and a BBC is reestablished.

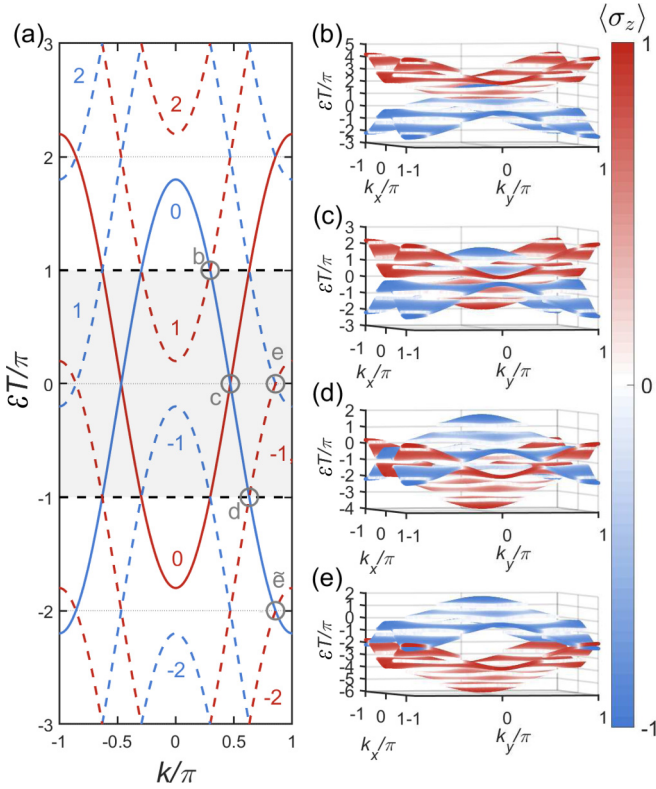


FIG. 3. (a) Quasienergy spectra along the cut of M - Γ - M with $k_x = k_y = k$, which connects high-symmetry points with $t_{so} = 0$. The blue and red lines represent spin-down and spin-up bands, respectively, and the solid (dashed) lines label the static (driving-induced) bands. Each band is labeled by its Floquet band index n , which denotes the shift of quasienergy $2n\pi/T$. Five band-touching points are highlighted by gray circles. For each point, the 2D spectra of the two intersecting bands are illustrated in the right column. Note that the band-touching points e and \bar{e} are identical due to the periodicity of FBZ. Other parameters used are $t_0/E_r = 0.5$, $t_{so}/E_r = 0.25$, $T_1/T_2 = 3/2$, $\delta/E_r = 1$, and $T = \pi/E_r$.

We emphasize that under conditions 1 and 2 introduced in Sec. II, Floquet engineering does not affect the position and chirality of band contact points at topological phase transitions, and the Floquet topological invariants $\nu_{F,m}^\Lambda$ are just the repetition of their static counterparts ν^Λ in the quasienergy dimension. In particular, when the system has inversion symmetry as in the QAHE model, the characterization of Floquet topological phases requires only information about the four high-symmetry points. Compared to the winding number, which needs to consider the time dimension [19], the topological invariants proposed here are not only concise and clear in theory but also more feasible for experimental detection.

IV. EXPERIMENTAL DETECTION

For a QAHE model realized in cold atomic gases, the topological phase can be characterized by the information about BISs obtained via quench dynamics [35]. Depending on the location in momentum space, there are two types of BISs. One surrounds the Γ point and corresponds to ν^Γ , while the other

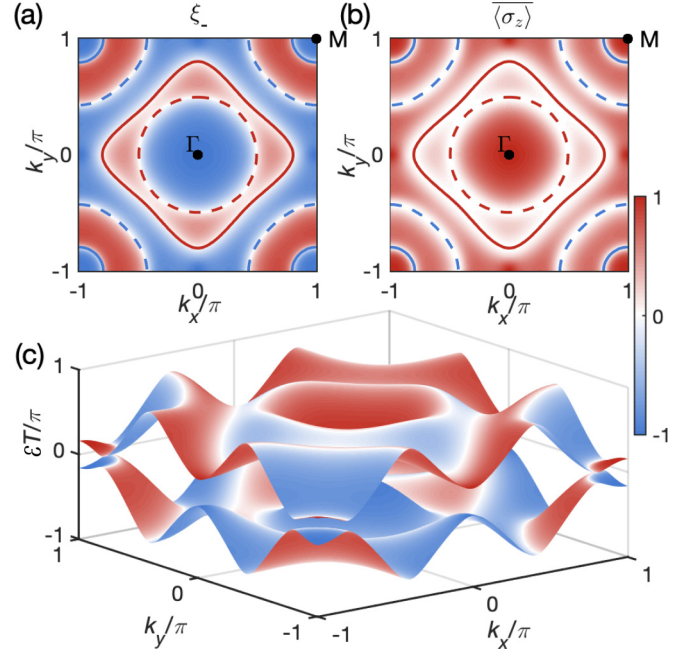


FIG. 4. Detection of topological invariants. (a) Equilibrium spin polarization of the lower band in phase iii shown in Fig. 2(a). (b) Stroboscopic time-averaged spin texture in the z direction for the same phase. The red (blue) lines indicate the BISs around the Γ (M) point, while the solid (dashed) lines label 0-BISs (π -BISs). (c) The Floquet band structure in the first FBZ for phase iii. Parameters used are $t_0/E_r = 0.5$, $t_{so}/E_r = 0.3$, $\delta/E_r = 0.8$, $T_1/T_2 = 3/2$, and $T = \pi/E_r$.

circles the M point and corresponds to ν^M . In a periodically driven system, the topological invariants are extended to four parameters $\nu_{F,m}^\Lambda$, each corresponding to a distinctive type of BIS, where $\Lambda = \{\Gamma, M\}$ labels which high-symmetry point a BIS surrounds and $m = \{0, \pi\}$ describes in which gap it lies.

Taking phase iii in Fig. 2(a) as an example, the spin polarization $\xi_-(\mathbf{k})$ of the lower Floquet band is shown in Fig. 4(a). We can see that there are two BISs around the M point and two around the Γ point in the 1BZ. The information about BISs can be determined by quench dynamics of a fully polarized initial state $|\uparrow\rangle$ [41]. For the periodically driven system, we need to detect the spin dynamics at the time of integer multiple periods, and the location of BISs can be determined as the location of zero stroboscopic time-averaged spin polarization along the z direction; that is, BISs equal $\{\mathbf{k} | \overline{\langle \sigma_z \rangle} = 0\}$, with

$$\overline{\langle \sigma_z \rangle} = \lim_{N \rightarrow \infty} \frac{1}{N} \sum_{\ell=0}^{N-1} \langle \sigma_z(\mathbf{k}, t = \ell T) \rangle, \quad (19)$$

as shown in Fig. 4(b). To distinguish which of the four BISs are lying in the 0-gap (denoted 0-BIS) and which are lying in the π -gap (π -BIS), we note that the stroboscopic quantum dynamics reads

$$\langle \sigma_z(\mathbf{k}, \ell T) \rangle = \frac{h_F^z(\mathbf{k})^2 + h_F^\perp(\mathbf{k})^2 \cos(2|\varepsilon(\mathbf{k})|\ell T)}{\varepsilon(\mathbf{k})^2}, \quad (20)$$

where h_F^\perp and h_F^z are the x - y and z components of the magnetic field \mathbf{h}_F in the effective Floquet Hamiltonian \mathcal{H}_F , respectively.

Thus, Floquet band structure $\varepsilon(\mathbf{k})$ can be mapped out by fitting the frequency of the dynamical evolution, and one can determine within which gap a given BIS resides. For the specific example of phase iii depicted in Fig. 4, we can easily identify one 0-BIS and one π -BIS around the Γ point, and one 0-BIS and one π -BIS around the M point. Therefore, the topological invariants can be extracted as $\nu_{F,0}^\Gamma = \nu_{F,\pi}^\Gamma = \nu_{F,0}^M = \nu_{F,\pi}^M = 1$, as shown in Fig. 2(b).

In addition to the method of fitting dynamical evolution, which usually requires a very high quality of experimental data, next, we propose another scheme to determine the topological invariants $\nu_{F,m}^\Delta$ by monitoring the sequence of BIS emergence with increasing driving period T . From Eqs. (17) and (18), we can conclude that the condition for a nontrivial topological invariant to emerge is $E_d^s - n\pi/T = 0$ for some integer n within the 1BZ. In the static limit of $T \rightarrow 0$, the only integer that may satisfy this condition is $n = 0$. Thus, in this limit if a BIS exists, it must lie in the 0-gap. As the driving period T is increased beyond a certain value, the choice of $n = 1$ can also fulfill the condition, and another BIS emerges in the π -gap. When T is further enhanced, more BISs with higher values of $n = 2, 3, \dots$ will be present, where the ones with odd (even) n reside in the 0-gap (π -gap). If two adjacent even numbers n and $n + 2$ can both satisfy the condition and support two 0-BISs, the value of $n + 1$ can also satisfy the condition and lead to a π -BIS lying in between. Thus, the 0- and π -BISs must emerge one by one with increasing T . Specifically, in the experiment we start from the static limit with $T \rightarrow 0$. If a BIS already exists, it must lie in the 0-gap. By slowly increase T , the next emerging BIS must be a π -BIS, and the following one is a 0-BIS and so forth. On the other hand, if the static system is in a topologically trivial phase with no BIS, the first emerging BIS within increasing T must reside in the π -gap, and the following ones can be determined accordingly. Thus, by recoding the emerging sequence of BISs and their locations in momentum space, we can extract the full information about BISs and their corresponding topological invariants. Taking phase iii as an example, the four BISs depicted in Fig. 4 are placed in the order of π -0- π -0 from the Γ to M points.

Compared with other methods for detecting the topological features of Floquet topological phases using information about BISs [30], we stress that the two schemes proposed here require only the stroboscopic measurement of the z polarization $\langle \sigma_z \rangle$, not the entire spin texture, which also includes $\langle \sigma_x \rangle$ and $\langle \sigma_y \rangle$ and usually requires more complicated procedures in experiments [42].

V. SUMMARY

We studied in this paper the characterization of Floquet topological phases in periodically driven systems, where the instantaneous Hamiltonian in the driving sequence preserves all symmetries of the static model such that the effective Floquet system also inherits the same symmetries. In such cases, a type-II anomalous Floquet topological (AFT-II) phase can exist, featuring nontrivial counterpropagating edge modes, which cannot be described by the Chern number or winding number of the Floquet bands. By assuming that the Floquet bands cross at the same location and acquire the same chirality as in the static model, we introduced a framework to obtain a complete characterization of Floquet topological phases, including the AFT-II phase, by extending the definition of topological invariants in static systems. Since the band-touching points are usually determined by symmetries, we emphasize that the conditions to validate the proposed framework are often naturally satisfied for the driving scheme considered here.

To give an example, we considered a quantum anomalous Hall effect (QAHE) model in a two-dimensional square lattice. When subjected to periodic driving with all symmetries preserved, the system can host an AFT-II phase with robust counterpropagating edge modes but a Chern number and winding number equal to zero. Owing to the particle-hole symmetry, this phase is a strong topological phase. Other symmetries guarantee that the bands can cross only at high-symmetry points with the same chirality. Using the scheme proposed here, we showed that all topological phases, including the strong topological AFT-II phase, can be well characterized by a set of topological invariants associated with these high-symmetry points. Finally, we suggested some experimental proposals to detect these topological invariants using quench dynamics in cold atomic gases in optical lattices. Since the periodically driven QAHE model and the measurement of quench dynamics have already been realized in experiments, our proposed theory can be readily implemented.

ACKNOWLEDGMENTS

We thank the Beijing Natural Science Foundation (Grant No. Z180013), the National Natural Science Foundation of China (Grant No. 12074428), the National Key R&D Program of China (Grant No. 2018YFA0306501), and the China Postdoctoral Science Foundation (Grants No. BX20200379 and No. 2021M693478) for support.

-
- [1] D. J. Thouless, M. Kohmoto, M. P. Nightingale, and M. den Nijs, Quantized Hall Conductance in a Two-Dimensional Periodic Potential, *Phys. Rev. Lett.* **49**, 405 (1982).
 - [2] X.-G. Wen, Topological orders in rigid states, *Int. J. Mod. Phys. B* **04**, 239 (1990).
 - [3] M. Hafezi, E. A. Demler, M. D. Lukin, and J. M. Taylor, Robust optical delay lines with topological protection, *Nat. Phys.* **7**, 907 (2011).
 - [4] Y. Yang, Y. F. Xu, T. Xu, H.-X. Wang, J.-H. Jiang, X. Hu, and Z. H. Hang, Visualization of a Unidirectional Electromagnetic Waveguide Using Topological Photonic Crystals Made of Dielectric Materials, *Phys. Rev. Lett.* **120**, 217401 (2018).
 - [5] C.-Y. Ji, G.-B. Liu, Y. Zhang, B. Zou, and Y. Yao, Transport tuning of photonic topological edge states by optical cavities, *Phys. Rev. A* **99**, 043801 (2019).

- [6] A. Blanco-Redondo, B. Bell, D. Oren, B. J. Eggleton, and M. Segev, Topological protection of biphoton states, *Science* **362**, 568 (2018).
- [7] J. E. Moore, The birth of topological insulators, *Nature (London)* **464**, 194 (2010).
- [8] A. P. Schnyder, S. Ryu, A. Furusaki, and A. W. W. Ludwig, Classification of topological insulators and superconductors in three spatial dimensions, *Phys. Rev. B* **78**, 195125 (2008).
- [9] A. Kitaev, Periodic table for topological insulators and superconductors, in *Advances in Theoretical Physics: Landau Memorial Conference*, AIP Conf. Proc. No. 1134 (AIP, Melville, NY, 2009), p. 22.
- [10] X. Chen, Z.-C. Gu, Z.-X. Liu, and X.-G. Wen, Symmetry protected topological orders and the group cohomology of their symmetry group, *Phys. Rev. B* **87**, 155114 (2013).
- [11] X. Chen, Z.-C. Gu, Z.-X. Liu, and X.-G. Wen, Symmetry-protected topological orders in interacting bosonic systems, *Science* **338**, 1604 (2012).
- [12] X.-L. Qi and S.-C. Zhang, Topological insulators and superconductors, *Rev. Mod. Phys.* **83**, 1057 (2011).
- [13] M. König, S. Wiedmann, C. Brüne, A. Roth, H. Buhmann, L. W. Molenkamp, X.-L. Qi, and S.-C. Zhang, Quantum spin Hall insulator state in HgTe quantum wells, *Science* **318**, 766 (2007).
- [14] D. Hsieh, D. Qian, L. Wray, Y. Xia, Y. S. Hor, R. J. Cava, and M. Z. Hasan, A topological Dirac insulator in a quantum spin Hall phase, *Nature (London)* **452**, 970 (2008).
- [15] A. Altland and M. R. Zimbauer, Nonstandard symmetry classes in mesoscopic normal-superconducting hybrid structures, *Phys. Rev. B* **55**, 1142 (1997).
- [16] C.-K. Chiu, J. C. Y. Teo, A. P. Schnyder, and S. Ryu, Classification of topological quantum matter with symmetries, *Rev. Mod. Phys.* **88**, 035005 (2016).
- [17] Y. Hatsugai, Chern Number and Edge States in the Integer Quantum Hall Effect, *Phys. Rev. Lett.* **71**, 3697 (1993).
- [18] X.-L. Qi, Y.-S. Wu, and S.-C. Zhang, General theorem relating the bulk topological number to edge states in two-dimensional insulators, *Phys. Rev. B* **74**, 045125 (2006).
- [19] M. S. Rudner, N. H. Lindner, E. Berg, and M. Levin, Anomalous Edge States and the Bulk-Edge Correspondence for Periodically Driven Two-Dimensional Systems, *Phys. Rev. X* **3**, 031005 (2013).
- [20] M. Lababidi, I. I. Satija, and E. Zhao, Counter-propagating Edge Modes and Topological Phases of a Kicked Quantum Hall System, *Phys. Rev. Lett.* **112**, 026805 (2014).
- [21] T.-S. Xiong, J. Gong, and J.-H. An, Towards large-Chern-number topological phases by periodic quenching, *Phys. Rev. B* **93**, 184306 (2016).
- [22] R. Roy and F. Harper, Periodic table for Floquet topological insulators, *Phys. Rev. B* **96**, 155118 (2017).
- [23] H. Liu, T.-S. Xiong, W. Zhang, and J.-H. An, Floquet engineering of exotic topological phases in systems of cold atoms, *Phys. Rev. A* **100**, 023622 (2019).
- [24] M. S. Rudner and N. H. Lindner, Band structure engineering and non-equilibrium dynamics in Floquet topological insulators, *Nat. Rev. Phys.* **2**, 229 (2020).
- [25] M. Umer, R. W. Bomantara, and J. Gong, Counterpropagating edge states in Floquet topological insulating phases, *Phys. Rev. B* **101**, 235438 (2020).
- [26] Y.-G. Peng, C.-Z. Qin, D.-G. Zhao, Y.-X. Shen, X.-Y. Xu, M. Bao, H. Jia, and X.-F. Zhu, Experimental demonstration of anomalous Floquet topological insulator for sound, *Nat. Commun.* **7**, 13368 (2016).
- [27] S. Mukherjee, A. Spracklen, M. Valiente, E. Andersson, P. Öhberg, N. Goldman, and R. R. Thomson, Experimental observation of anomalous topological edge modes in a slowly driven photonic lattice, *Nat. Commun.* **8**, 13918 (2017).
- [28] L. J. Maczewsky, J. M. Zeuner, S. Nolte, and A. Szameit, Observation of photonic anomalous Floquet topological insulators, *Nat. Commun.* **8**, 13756 (2017).
- [29] K. Wintersperger, C. Braun, F. N. Ünal, A. Eckardt, M. D. Liberto, N. Goldman, I. Bloch and M. Aidelsburger, Realization of an anomalous Floquet topological system with ultracold atoms, *Nat. Phys.* **16**, 1058 (2020).
- [30] L. Zhang, L. Zhang, and X.-J. Liu, Unified Theory to Characterize Floquet Topological Phases by Quench Dynamics, *Phys. Rev. Lett.* **125**, 183001 (2020).
- [31] I. C. Fulga and M. Maksymenko, Scattering matrix invariants of Floquet topological insulators, *Phys. Rev. B* **93**, 075405 (2016).
- [32] F. Nathan and M. S. Rudner, Topological singularities and the general classification of Floquet-Bloch systems, *New J. Phys.* **17**, 125014 (2015).
- [33] Z. Wu, L. Zhang, W. Sun, X.-T. Xu, B.-Z. Wang, S.-C. Ji, Y. Deng, S. Chen, X.-J. Liu, and J.-W. Pan, Realization of two-dimensional spin-orbit coupling for Bose-Einstein condensates, *Science* **354**, 83 (2016).
- [34] W. Sun, B.-Z. Wang, X.-T. Xu, C.-R. Yi, L. Zhang, Z. Wu, Y. Deng, X.-J. Liu, S. Chen, and J.-W. Pan, Highly Controllable and Robust 2D Spin-Orbit Coupling for Quantum Gases, *Phys. Rev. Lett.* **121**, 150401 (2018).
- [35] W. Sun, C.-R. Yi, B.-Z. Wang, W.-W. Zhang, B. C. Sanders, X.-T. Xu, Z.-Y. Wang, J. Schmiedmayer, Y. Deng, X.-J. Liu, S. Chen, and J.-W. Pan, Uncover Topology by Quantum Quench Dynamics, *Phys. Rev. Lett.* **121**, 250403 (2018).
- [36] H. Sambe, Steady states and quasienergies of a quantum-mechanical system in an oscillating field, *Phys. Rev. A* **7**, 2203 (1973).
- [37] F. N. Ünal, B. Seradjeh, and A. Eckardt, How to Directly Measure Floquet Topological Invariants in Optical Lattices, *Phys. Rev. Lett.* **122**, 253601 (2019).
- [38] D. Sticlet, F. Piéchon, J.-N. Fuchs, P. Kalugin, and P. Simon, Geometrical engineering of a two-band Chern insulator in two dimensions with arbitrary topological index, *Phys. Rev. B* **85**, 165456 (2012).
- [39] J. E. Avron, L. Sadun, J. Segert, and B. Simon, Topological Invariants in Fermi Systems with Time-Reversal Invariance, *Phys. Rev. Lett.* **61**, 1329 (1988).
- [40] X.-J. Liu, K. T. Law, T. K. Ng, and P. A. Lee, Detecting Topological Phases in Cold Atoms, *Phys. Rev. Lett.* **111**, 120402 (2013).
- [41] L. Zhang, L. Zhang, S. Niu, and X.-J. Liu, Dynamical classification of topological quantum phases, *Sci. Bull.* **63**, 1385 (2018).
- [42] C.-R. Yi, L. Zhang, L. Zhang, R.-H. Jiao, X.-C. Cheng, Z.-Y. Wang, X.-T. Xu, W. Sun, X.-J. Liu, S. Chen, and J.-W. Pan, Observing Topological Charges and Dynamical Bulk-Surface Correspondence with Ultracold Atoms, *Phys. Rev. Lett.* **123**, 190603 (2019).